Journal of Sound and Vibration (2001) **241**(4), 693–716
doi:10.1006/jsvi.2000.3307, available online at http://www.idealibrary.com on IDEAL®

SINGLE-MODE VIBRATION SUPPRESSION FOR A BEAM–MASS–CART SYSTEM USING INPUT PRESHAPING WITH A ROBUST INTERNAL-LOOP COMPENSATOR

S. PARK

Mechatronics Research Team, Research Institute of Industrial Science and Technology (RIST), San 32, Hyoja-dong, Nam-ku, 790-330, Pohang, Korea. E-mail: sdpark@rist.re.kr

AND

B. K. KIM AND Y. YOUM

Robotics and Bio-Mechatronics Laboratory, Department of Mechanical Engineering, Pohang University of Science and Technology (POSTECH), San 31, Hyoja-dong, Nam-ku 790-784, Pohang, Korea

(*Received* 25 *April* 2000, *and in final form* 6 *September* 2000)

In this paper, single-mode vibration suppression of an elastic beam fixed on a moving cart and carrying a concentrated or moving mass is considered. A modified pulse sequence method with robust internal-loop compensator (RIC) is proposed to suppress single-mode residual vibration and to get accurate positioning of the beam–mass–cart system. The performance of the proposed input preshaping method is compared with that of the previous ones by both numerical simulations and experiments. Using the proposed method, it is possible to suppress initial vibration of the beam–mass–cart system carrying a concentrated mass. Accurate PTP positioning of the moving mass without residual vibration is also obtained experimentally by modifying the proposed pulse sequence method. Finally, the proposed input preshaping method is applied to the system for following square trajectories of the moving mass without residual vibration

1. INTRODUCTION

Recently, as the production type in industrial fields has been changed over to an order-made one, the function of automated warehouses has been being regarded as important. Automated warehouses are mainly built high on effective area to maximize the efficiency of space, and it is important to move the objects to the target position as fast as possible to minimize the production time. To this end, stacker cranes or reclaimers with high-rise structures of which height is over tens of meters are used.

When the reclaimers carry heavy loads, vibrational motion due to the flexibility of the beam structure is unavoidable, even though they have truss-structured beams. The vibration generated at the main beam lasts long and is not easily damped out. Therefore, it takes long time to move heavy loads using these kinds of transportation equipments without suppressing the vibration. In that case, it is necessary to suppress the vibration as well as to move the base cart to the target position.

Various kinds of feedback controllers have been developed to reduce the end-point vibration [1, 2]. However, feedback control systems require sensory devices such as strain

0022-460X/01/140693 + 24 $35.00/0

gauges, accelerometers and/or CCD cameras to measure vibration, which are difficult to use in many cases of industrial implementations. Input preshaping method alters the shape of command of the actuator to reduce residual vibration. Therefore, it does not need sensory devices, and is relatively simple to implement. Input preshaping technique can also be used as reference input of feedback controllers.

Input preshaping technique is proposed first by Smith [3]. He showed that the posicast control technique which divided a step input into two small-step inputs with time delay resulted in reduced settling time. This method, however, was no robust with respect to the change of frequency modes. Aspinwall [4] showed a pulse-shaping technique utilizing a finite Fourier series expression to attenuate residual dynamic response in elastic systems and then selected the Fourier coefficients to depress the residual response spectrum in desired regions. Swigert [5] evaluated the shapeed torque technique for the control of terminal boundary conditions and synthesized torque waveforms that were relatively insensitive to variations in the plant parameters.

Meckl and Screening [6, 7] developed a multiswitch bang–band functions to achieve time-optimal control and derived a series of harmonics of ramped sinusoids which control the vibration throughout the move to eliminate residual vibration of a robot arm. They also presented a control scheme to reduce both the move time and settling time of a typical flexible dynamic system utilizing a state-variable feedback controller modified with the addition of a suitably shaped feedforward forcing function [8]. Further, a set of shaped force profiles constructed from a versine function and its harmonics with coefficient to minimize the excitation energy at the velocity-limited system's first natural frequency during motion were developed by them [9].

Singer and Seering [10] tried to reduce residual vibration of a manipulator by reshaping the rectangular input pulse utilizing an acausal filter so that it contains no frequency components in the vicinity of the first two structural resonances of the manipulator. However, the technique had some limitation to generate complicated input in implementation. They also presented the input preshaping method with robustness to errors in system natural frequency and in system damping utilizing impulse inputs [11–13]. Hyde and Seering [14] extended the impulse shaping technique to suppress multiple-mode vibration.

Bhat and Miu [15] evaluated an open-loop residual vibration suppression controller utilizing the fact that the magnitude of finite-time Laplace transform has the value of zero at poles of the system. Tuttle and Seering [16] illustrated an optimal input shapers to suppress multiple-mode vibration using zero-placement technique in the discrete domain. Singh *et al.* [17] designed a sliding-mode/shaped-input controller for a flexible/rigid robots. Teo *et al.* [18] presented inputs in the form of pulse sequences which possessed robustness to the variations in the parameters of the system to reduce the residual vibration to overhead crane.

In this paper, a modified pulse sequence method with a robust internal-loop compensator (RIC) is proposed to reduce single-mode residual vibration of the beam–mass–cart system. The performance of the proposed input preshaping method is compared with that by previous methods by Teo *et al.* [18] and Singer and Seering [11]. The vibration suppression performance of the proposed pulse sequence method for the point-to-point (PTP) motion of the beam–mass–cart system with a concentrated mass is verified by experiments. The proposed method is implemented to suppress initial vibration of the beam–mass–cart system carrying a concentrated mass. Accurate PTP positioning and following square trajectories of the moving mass without residual vibration are also obtained experimentally by modifying the proposed pulse sequence method.

2. THE BEAM–MASS–CART SYSTEM

Reclaimers in automated warehouses can be simplified as a Bernoulli–Euler beam fixed on a moving cart and carrying a moving mass as shown in Figure 1. The equations of motion and the boundary conditions for this beam–mass–cart system can be written as follows [19]:

$$m\ddot{x} + \int_0^l \{[\rho_0 + m\delta(y-h)](\ddot{x}+\ddot{w})(\ddot{x}+\ddot{w}) + m\delta(y-h)[\ddot{h}w' + 2\dot{h}\dot{w}' + \dot{h}^2 w'']\}\,\mathrm{d}y = f_1(t) \tag{1}$$

$$EIw'''' + [\rho_0 + m\delta(y-h)](\ddot{x}+\ddot{w}) + m\delta(y-h)[\ddot{h}w' + 2\dot{h}\dot{w}' + \dot{h}^2 w''] = 0 \tag{2}$$

$$m\{\ddot{h} + (\ddot{x} + \ddot{w}_h + \dot{h}^2 w_h'' + 2\dot{h}\dot{w}_h')w_h' + g\} = f_2(t) \tag{3}$$

and

$$w(0,t) = w'(0,t) = EIw''(l,t) = EIw'''(l,t) = 0, \tag{4}$$

where M is the mass of the cart, ρ_0 is the mass per unit length of the unloaded beam, m is the mass of the lumped mass, $\delta(y-h)$ is the *Dirac delta-function*, EI is the flexural rigidity of the beam, l is the length of the beam, x is the position of the cart, and $w(y,t)$ is the deflection of the beam at y.

Natural frequencies of the beam–mass–cart system in Figure 1 are represented as

$$\omega_i^2 = \frac{EIk_i^4}{\rho_0}, \tag{5}$$

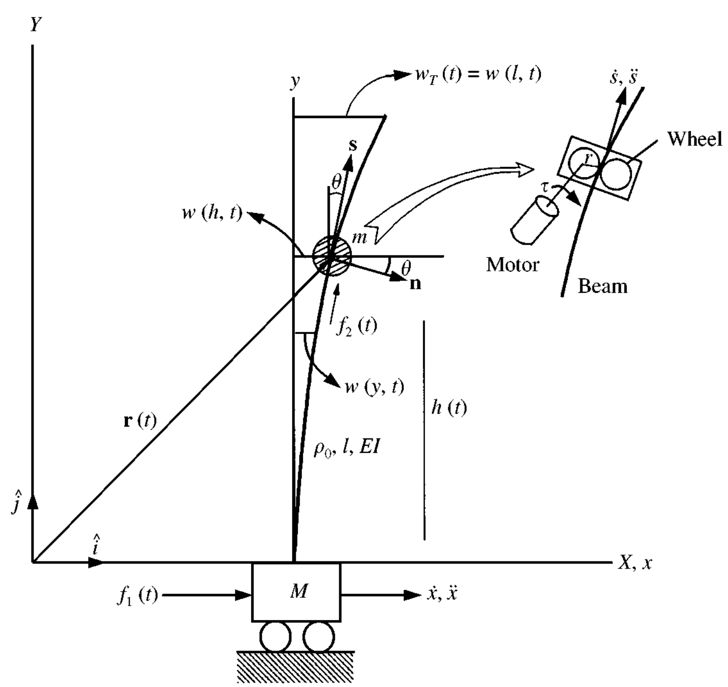

Figure 1. The beam–mass–cart system considered.

where k_i are the roots of the frequency equation changed along the weight ratios of the beam–mass–cart system and the position of the moving mass as follows [20]:

$$\begin{aligned}
&1 + \cos\xi\cosh\xi \\
&\quad + \frac{r_1}{4}[\cos\xi\cosh(\xi - 2\eta) + \cos(\xi - 2\eta)\cosh\xi + \sin\xi\sinh(\xi - 2\eta) \\
&\quad - \sin(\xi - 2\eta)\sinh\xi + 2\cos\xi\cosh\xi + 4\cos\eta\cosh\eta] \\
&\quad + \frac{r^2}{\xi}(\sin\xi\cosh\xi + \cos\xi\sinh\xi) \\
&\quad + \frac{r_3\xi}{4}[2\sin(\xi - \eta)\cosh(\xi - \eta) + 2\cos\eta\sinh\eta - 2\cos(\xi - \eta)\sinh(\xi - \eta) \\
&\quad - 2\sin\eta\cosh\eta + \cos(\xi - 2\eta)\sinh\xi - \sin\xi\cosh(\xi - 2\eta) \\
&\quad + \cos\xi\sinh\xi - \sin\xi\cosh\xi] = 0,
\end{aligned} \tag{6}$$

where $r_1 = m/M$, $r_2 = m_b/M$, $r_3 = m/m_b$, $m_b = \rho_o l$, $\xi = kl$ and $\eta = kh$.

3. VIBRATION SUPPRESSION CONTROLLER

3.1. PREVIOUS INPUT PRESHAPING METHODS

Impulse shaping command input by Singer and Seering [12] is obtained by convolution of the "bang–bang" control input and impulse trains as shown in Figure 2. The impulse trains which are robust to system natural frequencies and damping coefficient can be obtained as in Figure 2. In Figure 2,

$$\Delta T = \frac{\pi}{\omega_1\sqrt{1 - \zeta^2}}, \tag{7}$$

where ω_1(rad/s) is the fundamental natural frequency of the beam–mass–cart system, $K = \exp(-\zeta\pi/\sqrt{1 - \zeta^2})$, where ζ is the damping coefficient of the flexible beam, and $\Delta t = V_{max}/a_{max}$ where a_{max} and V_{max} are the given maximum acceleration and velocity of the base cart respectively.

Figure 3 shows the six-pulse sequence with robustness by Teo *et al.* [18]. It is assumed that maximum acceleration and velocity and the target position are given. In Figure 3,

$$a = \frac{V_{max}}{4\Delta t} \tag{8}$$

and

$$\lambda = \mathrm{e}^{-\zeta\omega_1(L - 0{\cdot}5)T}, \tag{9}$$

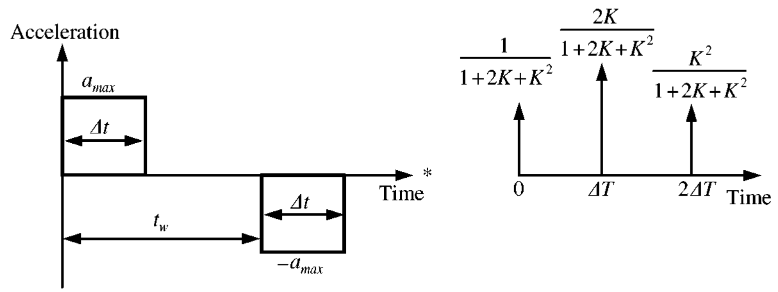

Figure 2. Three-impulse shaping method by Singer and Seering.

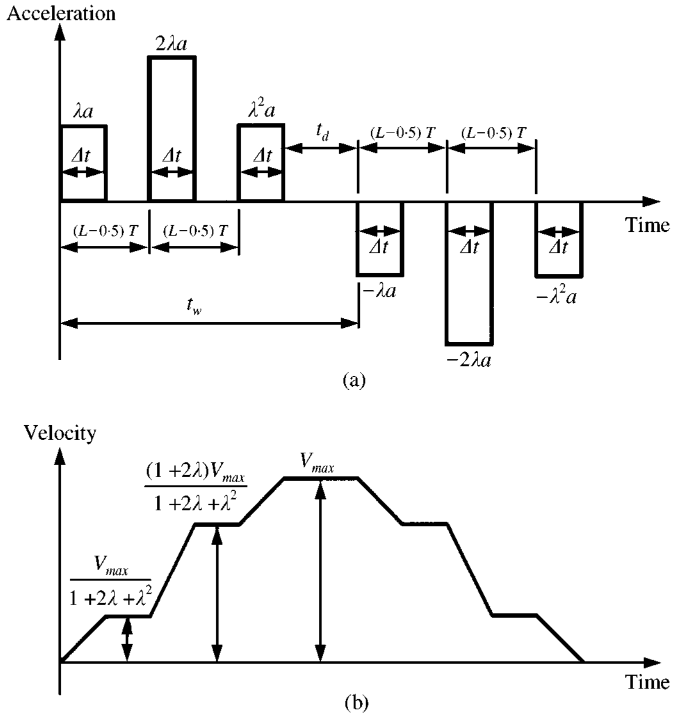

Figure 3. Six-pulse sequence with robustness by Teo *et al.*: (a) acceleration profile, (b) velocity profile.

where $T = 2\pi/\omega_1\sqrt{1-\zeta^2}$, and the integer L to determine the interval of each pulse is obtained as

$$L = \begin{cases} \operatorname{int}\left(\dfrac{V_{max}}{Ta_{max}} + 1{\cdot}5\right) & \text{if } \zeta \neq 0, \\[2ex] \operatorname{int}\left(\dfrac{V_{max}}{2Ta_{max}} + 1{\cdot}5\right) & \text{if } \zeta = 0, \end{cases} \tag{10}$$

and the duration of each pulse is determined as

$$\Delta t = \begin{cases} \dfrac{V_{max}}{a_{max}(1/2\lambda + 1 + 0{\cdot}5\lambda)} & \text{if } 2\lambda \geqslant 1, \\[2ex] \dfrac{V_{max}}{a_{max}(1 + 2\lambda + \lambda^2)} & \text{if } 2\lambda < 1. \end{cases} \tag{11}$$

The system reaches a maximum velocity at the end of the third pulse. The time taken to reach the target position x_f is given as

$$t_f = t_w + 2(L - 0{\cdot}5)T + \Delta t, \tag{12}$$

where $t_w = x_f/V_{max}$.

This method, however, fails to generate proper pulse sequence when $t_w < 2(L - 0{\cdot}5)T + \Delta t$. For example, the minimum time from the first pulse to the fourth one is $T + \Delta t$ when $L = 1$, and that may be larger than t_w if the target position, x_f, is relatively short and/or V_{max} is large. In this case, the pulses after the fourth one are superposed on the former ones. Furthermore, large acceleration commands with short time duration, especially at high natural frequencies, may bring about large tip deflection.

3.2. PROPOSED INPUT PRESHAPING METHOD FOR THE BEAM–MASS–CART SYSTEM CARRYING A FIXED MASS

The proposed pulse sequence method having robustness to system parameters is obtained by modifying the previous input shaping method as shown in Figure 4. The previous method determines the interval and duration time of each pulse with respect to the maximum acceleration, maximum velocity and target position. The proposed method determines the magnitude of acceleration with respect to the given maximum velocity and the final target position.

In Figure 4, the magnitude of acceleration to be applied to reach target position, x_f, is obtained as

$$a^* = \frac{x_f}{12\lambda[(L - 0{\cdot}5)T^2]}, \tag{13}$$

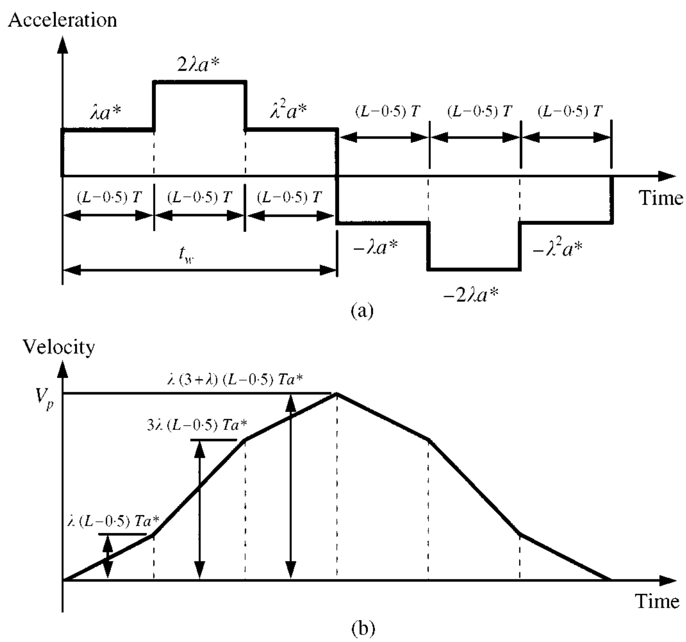

Figure 4. Proposed pulse sequence with robustness: (a) acceleration profile, (b) velocity profile.

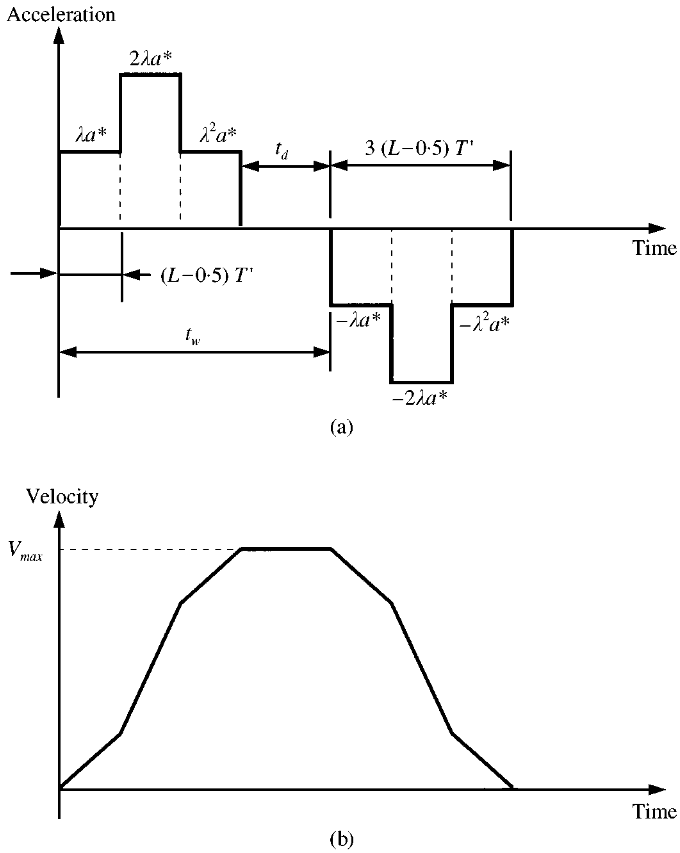

Figure 5. Proposed pulse sequence with robustness when $V_p \geqslant V_{max}$: (a) acceleration profile, (b) velocity profile.

and in this case,

$$t_w = 3(L - 0{\cdot}5)T. \tag{14}$$

The peak velocity of the base cart is given as

$$V_p = \frac{(3+\lambda)x_f}{12(L-0{\cdot}5)T}. \tag{15}$$

If the system natural frequency is changed and T is changed to T', and consequently, if $V_p \geqslant V_{max}$, then the duration time of maximum velocity must be determined to reach at the target position as seen in Figure 5. In this case, since

$$x_f = 2\lambda(L - 0{\cdot}5)T'a^* \left[6(L-0{\cdot}5)T' + \frac{3+\lambda}{2} t_d \right] \tag{16}$$

and

$$V_{max} = \lambda(3+\lambda)(L-0{\cdot}5)T'a^*, \tag{17}$$

the magnitude of acceleration to be applied to reach the target position, x_f, is given as

$$a^* = \frac{V_{max}}{\lambda(3+\lambda)(L-0{\cdot}5)T'}. \tag{18}$$

Since the duration time t_d is given as

$$t_d = \frac{x_f}{V_{max}} - \frac{12(L-0{\cdot}5)T'}{3+\lambda}, \tag{19}$$

t_w is determined as

$$t_w = \frac{x_f}{V_{max}} - \frac{3(1-\lambda)(L-0{\cdot}5)T'}{4(3+\lambda)}. \tag{20}$$

3.3. INPUT PRESHAPING FOR A MOVING MASS

When the beam–mass–cart system considered in this study carries a mass load from a position to the other position in the X–Y plane in Figure 1, the vibration characteristics of the system varies with respect to the change of the dynamics of the moving mass. To cancel out the time-varying vibration characteristics of the beam–mass–cart system carrying a moving mass, for the PTP positioning of the moving mass, the horizontal and the vertical motion of the system can be decoupled by considering the input preshaping method shown in Figure 6.

If the target is positioning the moving mass from $(0, h_1)$ to (x_f, h_2) in the $X - Y$ plane, the procedure for this target is composed of as follows:

1. accelerate the base cart without residual vibration after $t = 3(L - 0{\cdot}5)T_1$ using the proposed input preshaping with the period T_1 which is compatible to the initial vertical position of the moving mass, h_1;
2. move the moving mass from h_1 to h_2 when the base cart moves with constant velocity;
3. decelerate the base cart without residual vibration after $t = 3(L - 0{\cdot}5)(T_1 + T_2) + t_d$ using the proposed input preshaping with the period T_2 which is compatible to the final position of the moving mass, h_2.

Therefore, the moving mass can be positioned in $3(L - 0{\cdot}5)(T_1 + T_2) + t_d$, where t_d is the time necessary to move the moving mass from h_1 to h_2. In general, in real applications, the distance from 0 to x_f is longer than that from h_1 to h_2. Thus, the moving mass can move to the target position during the base cart moves with maximum speed.

The design of the force profile for the PTP positioning of the moving mass from the point $(0, h_1)$ to (x_f, h_2) is simple. Figure 7 shows the acceleration and the velocity profiles of the proposed method. According to the input preshaping method shown in Figure 7, if the target position x_f is given, then the acceleration which should be applied to the base cart to arrive at the target position is given as

$$a_1 = \frac{4x_f}{\lambda(L-0{\cdot}5)T_1}[2(11+\lambda)(L-0{\cdot}5)T_1 + 4(3+\lambda)t_d + 2(11+\lambda)(L-0{\cdot}5)T_2]^{-1}. \tag{21}$$

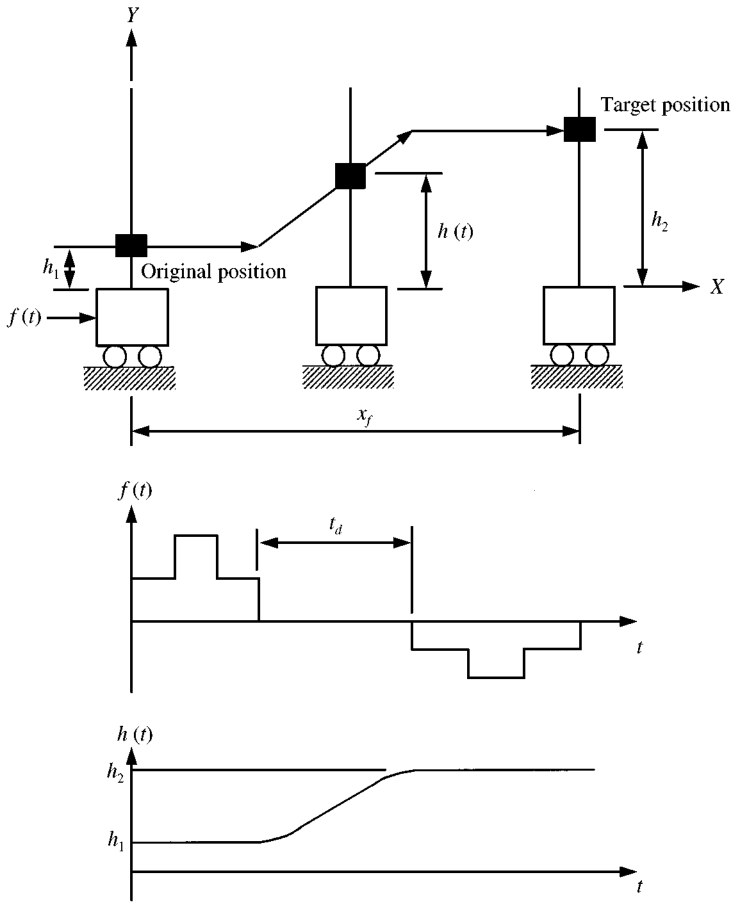

Figure 6. Input preshaping for the PTP positioning of the moving mass.

Since the total energy applied to accelerated the beam–mass–cart system must be equal to decelerate the system, i.e., $T_1 a_1 = T_2 a_2$, the magnitude of a_2 is given as

$$a_2 = \frac{T_1}{T_2} a_1. \tag{22}$$

4. NUMERICAL SIMULATIONS

4.1. PTP WITH A CONCENTRATED MASS

Numerical simulations are carried out to compare the performance of the proposed input preshaping method with that by the previous ones. The beam–mass–cart system in Figure 1 and system parameters in Table 1 were used in the simulations. The maximum force applied to the cart and the maximum velocity of the cart are limited to $F_{max} = 20$ N and $V_{max} = 0{\cdot}4$ m/s, respectively, and $x_f = 0{\cdot}4$ m. For the given conditions, $t_w = 1$ s, $M_t = 15{\cdot}182$ kg, and thus $a_{max} = 1{\cdot}2359$ m/s^2.

Figures 8 and 9 show the shaped input forces, velocity profiles, position profiles of the cart, and deflections when $h = 0{\cdot}4$ and $0{\cdot}6$ respectively. When $h = 0{\cdot}4$, the fundamental

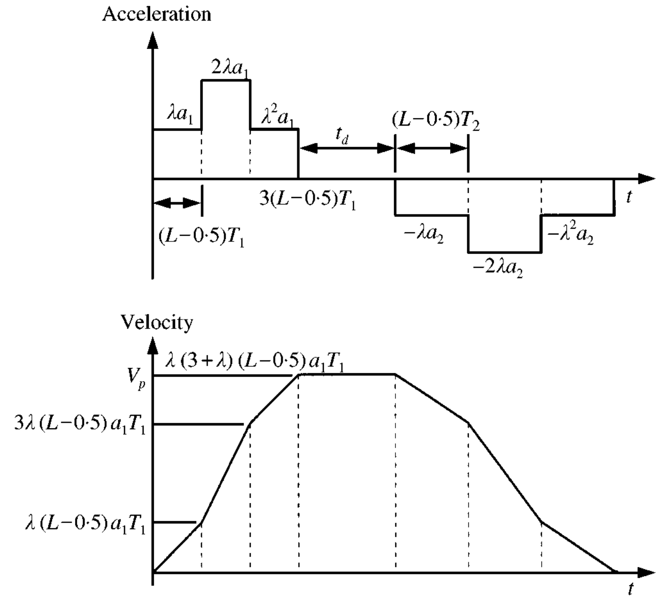

Figure 7. The proposed pulse sequence method for the point-to-point motion with a moving mass: (a) acceleration profile, (b) velocity profile.

TABLE 1

System parameters for numerical simulations

Parameters	Value
Mass of cart, M	10·0 kg
Mass of concentrated mass, m	5·0 kg
Length of elastic beam, l	1·0 m
Mass per unit length, ρ_0	1·182 kg/m
Young's module, E	$2{\cdot}07 \times 10^{11}$ N/m^2
Area moment of inertia, I	$1{\cdot}125 \times 10^{-10}$ m^4
Damping ratio, ζ	0

natural frequency $\omega_1 = 2{\cdot}1016$ Hz, and thus the period of the first vibration mode $T = 0{\cdot}4758$ s. In this case, the maximum driving force for the base cart by the proposed method is smaller than those by other ones as seen in Figure 8(a). Velocity profile of the cart by proposed input shaping method is simpler than others as seen in Figure 8(b). The total time taken to reach the target position is: Teo's method < Proposed method < Singer's method as seen in (c). The deflection at $y = h$ and the tip deflection are: Proposed method < Singer's method < Teo's method as seen in Figure (8d) and 8(e).

When $h = 0{\cdot}6$, the fundamental natural frequency $\omega_1 = 1{\cdot}4177$ Hz, and thus the period of the first vibration mode $T = 0{\cdot}7054$. In this case, the total time taken to reach the target is: Teo's method < Singer's method < Proposed method as seen in Figure 9(c). However, the deflection at $y = h$ and the tip deflection are: Proposed method < Singer's method < Teo's method as seen in Figure 9(d) and 9(e).

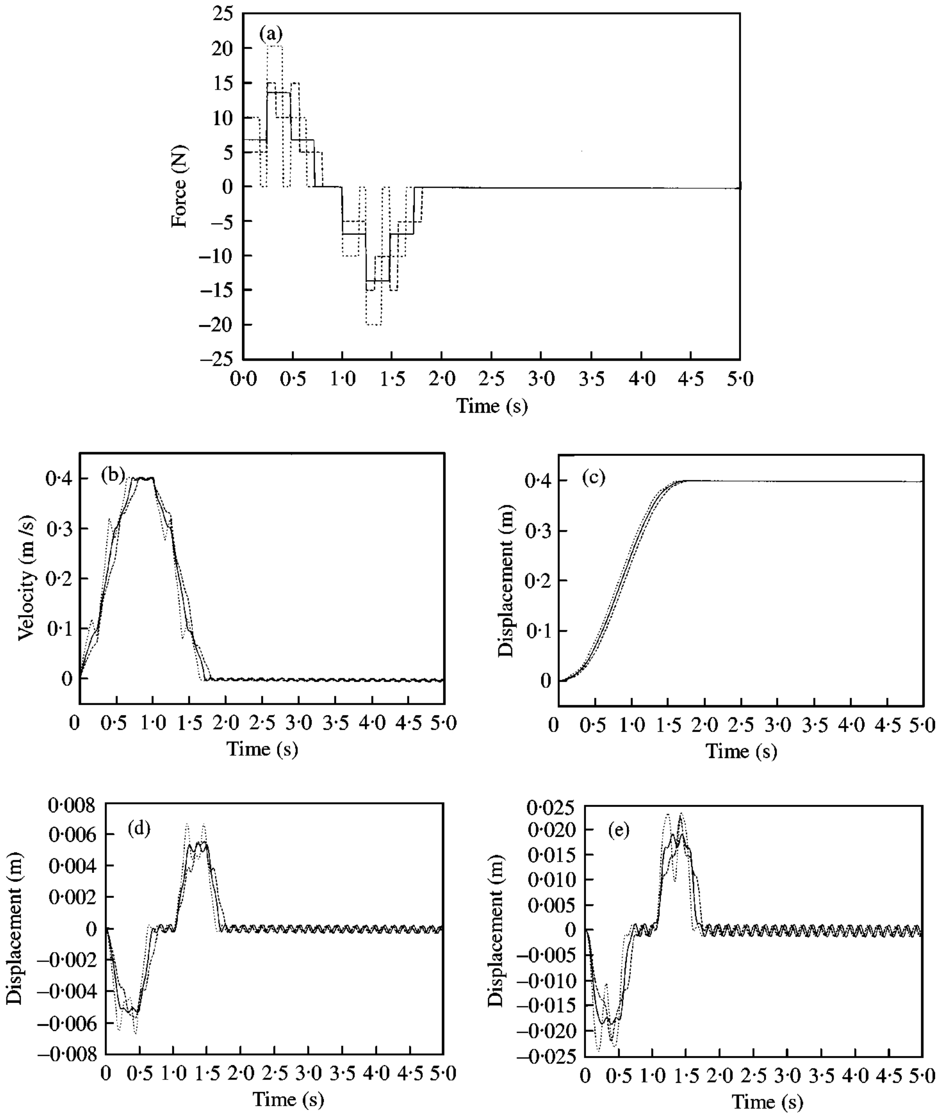

Figure 8. Numerical comparison of the three methods when $h = 0{\cdot}4$, $V_{max} = 0{\cdot}4$ m/s and $x_f = 0{\cdot}3$ m: (a) forcing function, (b) velocity of cart, (c) position of cart, (d) deflection at $y = h$, (e) tip deflection: ——, by proposed method; - - -, by Singer's method; ······, by Teo's method.

4.2. PTP WITH A MOVING MASS

Numerical simulations for the PTP positioning of the moving mass from (x_1, h_1) to (x_2, h_2) in the X–Y plane was carried out. System parameters for the simulations are listed in Table 1 except that the dimension of the flexible beam is 50 mm$(W) \times 3$ mm$(t) \times 1$ m(L), and thus, $\rho_0 = 1{\cdot}17$ kg/m. The task is to move the moving mass from (0, 0·4) to (0·4, 0·6) in the X–Y plane.

Figure 10 shows the simulated response of the beam–mass–cart system when the proposed input preshaping method is used. The first pulse sequence makes the cart to start

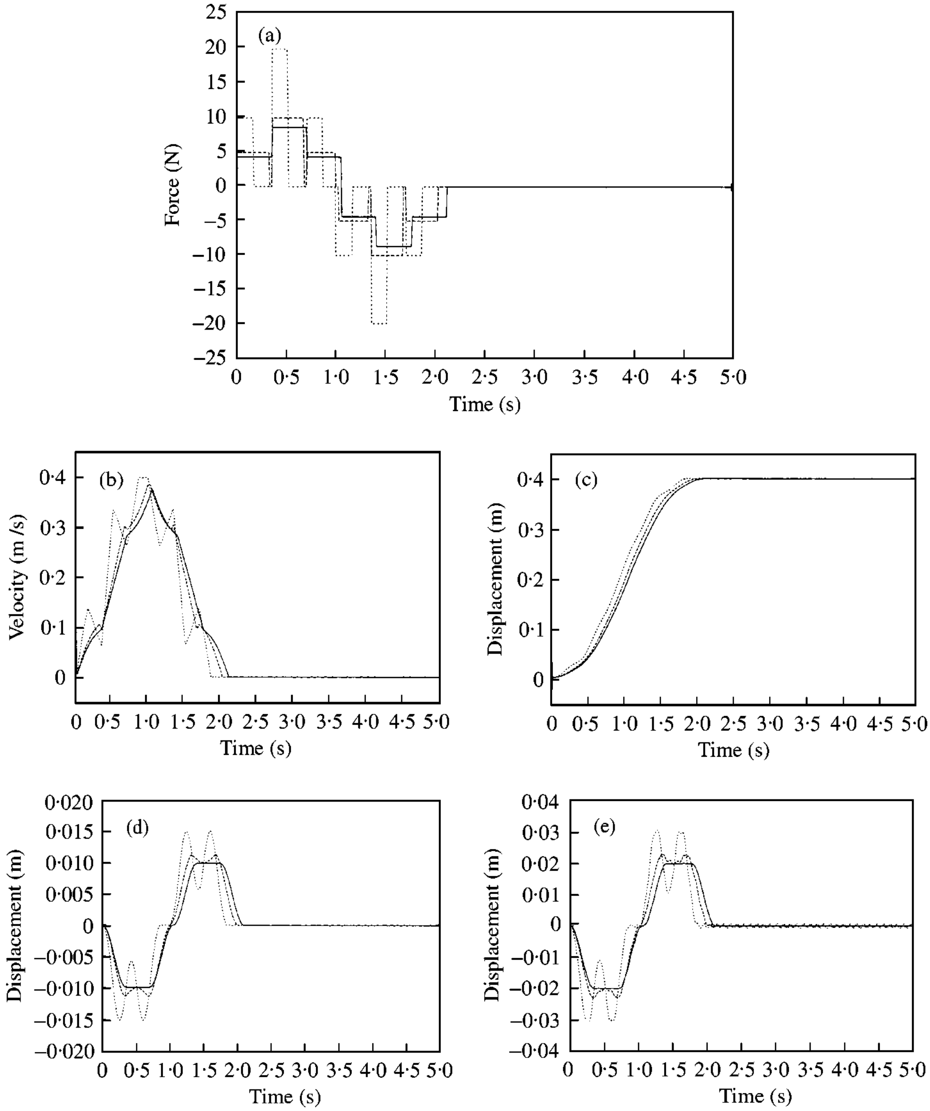

Figure 9. Numerical comparison of the three methods when $h = 0{\cdot}6$, $V_{max} = 0{\cdot}4$ m/s and $x_f = 0{\cdot}4$ m: (a) forcing function, (b) velocity of cart, (c) position of cart, (d) deflection at $y = h$, (e) tip deflection: ——, by proposed method; - - -, by Singer's method; ······, by Teo's method.

without residual vibration after $3T_1/2$, and the second pulse sequence continued during $3T_2/2$ makes the base cart to stop without residual vibration.

5. EXPERIMENTS

5.1. EXPERIMENTAL SET-UP

Figure 11(a) shows the experimental set-up. As seen in Figure 11(a), a thin flexible beam carrying a concentrated or a moving mass is clamped on the moving carriage of a linear

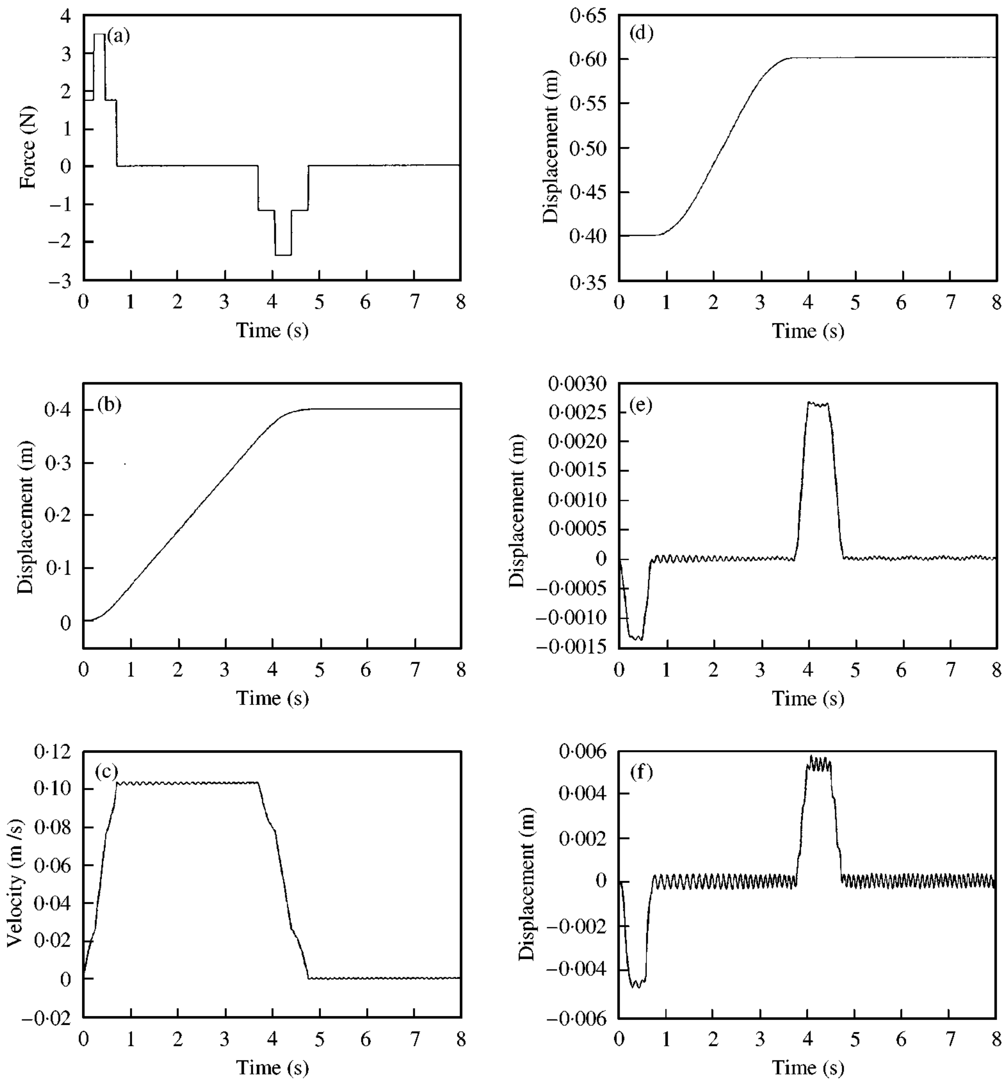

Figure 10. PTP positioning of the moving mass from $(X, Y) = (0, 0{\cdot}4)$, to $(0{\cdot}4, 0{\cdot}6)$ by the proposed input preshaping method: (a) shaped force, (b) cart position, (c) cart velocity, (d) moving mass position, (e) $w_h(t)$, (f) $w_T(t)$.

motor by a beam fixture. The linear motor used as the moving base is LEB-S-2-S made by ANORAD Corp. Schematics of the experimental set-up and brief explanations are shown in Figure 11(b). The moving mass moves along the flexible beam by two rubber-coated wheels driven by an AC servo motor and a reduction gear as seen in Figure 11(c). Strain gauges attached to the near bottom end of the elastic beam are used to measure the deflection of the beam. Table 2 shows the specification of the experimental set-up.

5.2. CONTROL WITH ROBUST INTERNAL-LOOP COMPENSATOR

The proposed pulse sequence was shaped without considering disturbances such as friction, etc. However, the linear motor used as the moving carriage shows a lot of

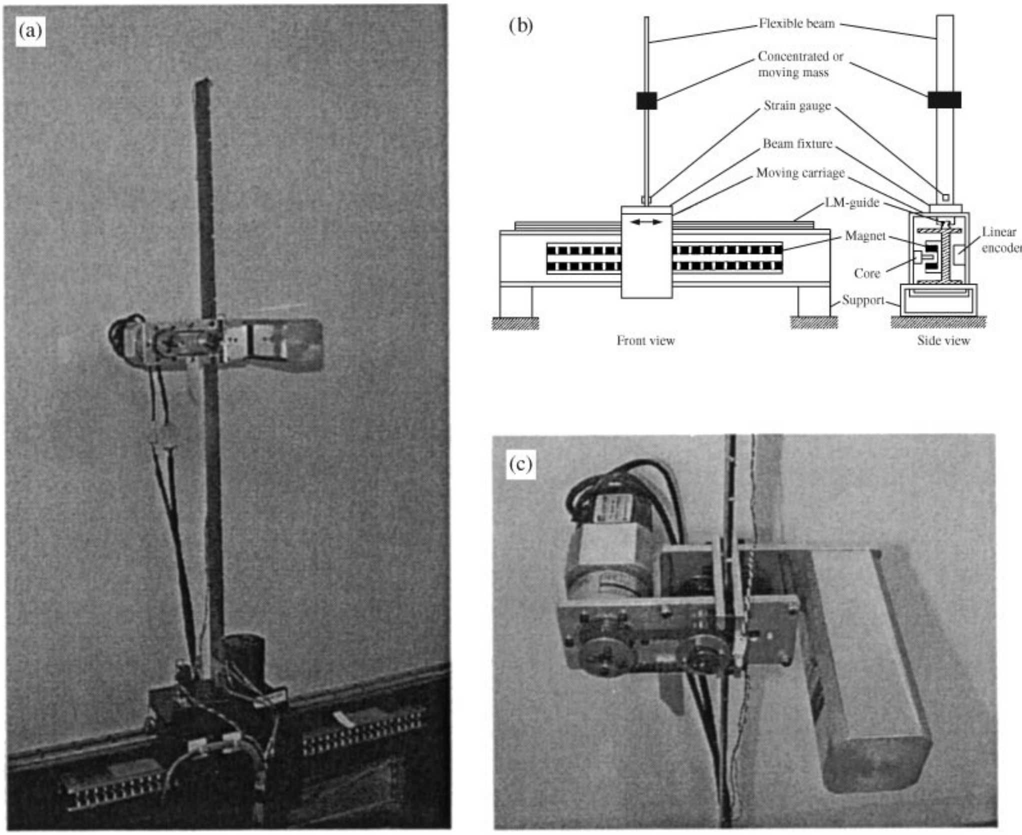

Figure 11. The experimental set-up: (a) photograph of the experimental set-up, (b) schematics of the experimental set-up, (c) photograph of the moving mass.

TABLE 2

Specifications of the experimental set-up

Moving base	Max. moving velocity	2·0 m/s
	Resolution of encoder	2 μm
	Mass of moving carriage	5·04 kg
	Mass of beam fixture	4·16 kg
Elastic beam	Dimension ($L \times W \times T$)	$1000 \times 50 \times 3{\cdot}8$ mm
	Mass per unit length, ρ_0	1·4776 kg/m
	Area moment of inertia, I	$2{\cdot}279 \times 10^{-10}$ m^4
	Young's modulus, E	$2{\cdot}07 \times 10^{11}$ N/m
Moving mass	Rated power of servo motor	100 W
	Rated torque of servo motor	0·32 Nm
	Gear reduction rate	10 : 1
	Total weight	5·4 kg

non-linearities including position-varying friction force. To compensate the non-linear disturbances, mainly the friction between the moving carriage and the LM-guide of the linear motor, the RIC [21] as seen in Figure 12 is used. The RIC makes the real plant to follow the trajectory of the plant model, an ideal one without disturbance, by the shaped command in spite of the distrubances.

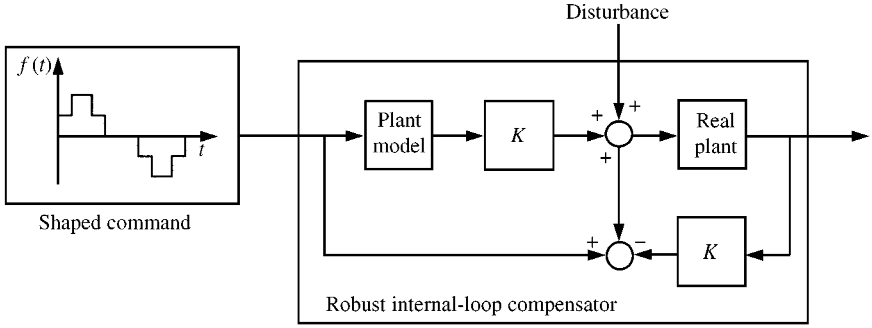

Figure 12. Block diagram of the controller using the proposed pulse sequence and the RIC.

5.3. PTP POSITIONING OF THE BEAM–MASS–CART SYSTEM WITH A CONCENTRATED MASS

The performance of the proposed input preshaping method for PTP positioning of the beam–mass–cart system with a concentrated mass is verified experimentally. For this purpose, the linear motor of the testbed was driven by the proposed control method, and the position of the moving carriage and the strain signal obtained from the root of the flexible beam are measured.

Figure 13 shows the shaped command by the proposed pulse sequence method and the system responses obtained from experiment when $m = 5$ kg, $h = 0{\cdot}5$ m, and $V_{max} = 0{\cdot}5$ m/s for $x_f = 10$, 20 and 40 cm respectively. In this experiment, the fundamental natural frequency of the beam–mass–cart system obtained from pre-experiment is given as $\omega_1 = 1{\cdot}797$ Hz, which is similar to the analytical result by equation (6) using the constrained method [20]. As seen in Figure 13, the base cart arrives at the given target position, and the first mode residual vibration disappears after the cart stops at the target position. In this experiment, the final time to arrive at the target position of all the cases is the same, it is $t_f = 3T$. The final time to arrive at the target position in this experiment is 1·6694 s.

The performance of the proposed input shaping method in vibration suppression of the beam–mass–cart system carrying a concentrated mass is compared with that by other methods, by Teo *et al.* and by Singer and Seering. In these experiments the maximum values of the shaped command, acceleration and velocities is limited in $F_{max} = 35$ N, $a_{max} = 1{\cdot}5$ m/s^2, and $V_{max} = 0{\cdot}5$ m/s respectively.

Figure 14 shows the experimental results of PTP positioning of the beam–mass–cart system carrying a concentrated mass when $m = 5$ kg, $h = 0{\cdot}5$ m and $x_f = 0{\cdot}4$ m. The fundamental natural frequency for all the method considered in these experiments is $\omega_1 = 1{\cdot}797$ Hz. As seen in Figure 14(a)–14(e), the force $f(t)$ applied to the cart and the maximum strain signal are: the proposed method < Singer' method < Teo's method. The steady state high-frequency strain signals by both Teo's and Singer's methods are larger than that by the proposed one. The time taken to reach the target position is: Teo's method < the proposed method < Singer's method as seen in Figure 14(g).

From Figure 14, it can be known that the higher mode residual vibration by the proposed method is smaller than that by others. Since all the input preshaping methods considered in this study can suppress only the first mode residual vibration, it is impossible to discuss the vibration suppression performance for higher mode residual vibration over the second mode. However, it can be thought that the proposed input preshaping method has more possibility to yield smaller higher mode residual vibration than the others because the change of the applied force and the velocity profile by the proposed method is smaller

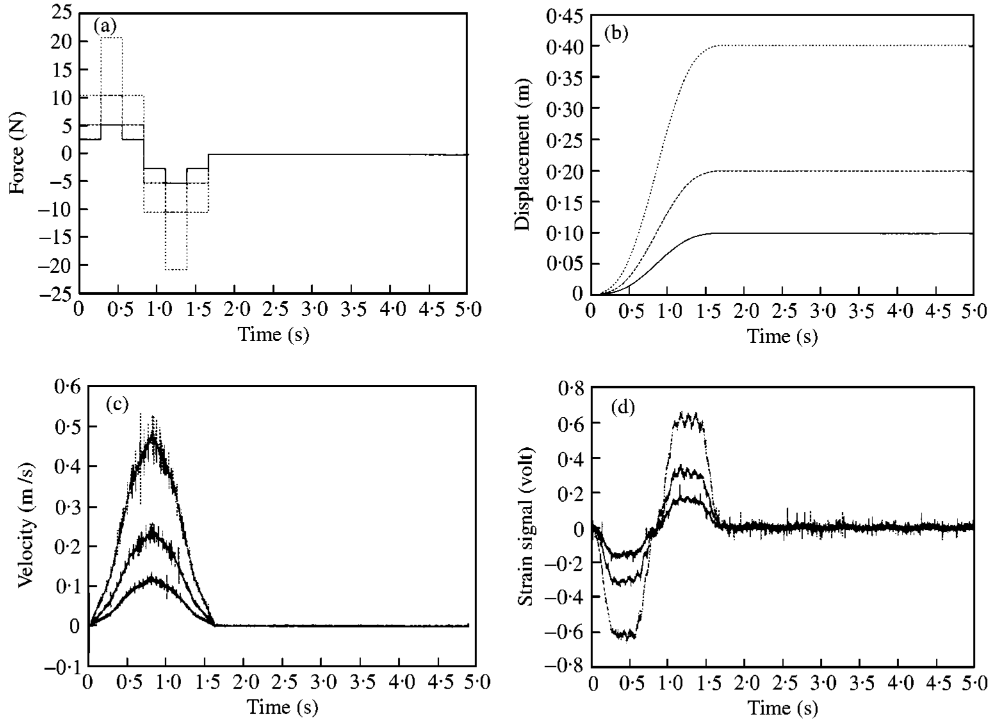

Figure 13. Shaped command and experimental response by proposed pulse sequence method when $m = 5$ kg, and $h = 0{\cdot}5$ m: (a) shaped force, (b) position of the base cart, (c) velocity of the base cart, (d) strain signal of the flexible beam. ——, $x_f = 10$ cm; - - -, $x_f = 20$ cm; ······, $x_f = 40$ cm.

and smoother, respectively, than the others. In this sense, Teo's method has the greatest chance to generate higher mode residual vibration among three methods although it shows the shortest operational time.

5.4. PTP POSITIONING OF THE BEAM–MASS–CART SYSTEM WITH A MOVING MASS

An experiment for the point-to-point (PTP) positioning of the moving mass in the X–Y plane was performed on the testbed using the proposed input preshaping method shown in Figure 6. The task is to position the moving mass from a point to the other point in the X–Y plane. The pulse sequence is designed as shown in Figure 7.

Figure 15 shows experimental results when the moving mass moves from $(X, Y) = (0, 0{\cdot}6)\, m$ to $(0{\cdot}4, 0{\cdot}4) m$. As seen in Figure 15, the base cart is accelerated by the first pulse sequence during $3(L - 0{\cdot}5)T_1$ and moves with constant velocity during t_d in Figure 7. The moving mass starts after $t = 3(L - 0{\cdot}5)T_1$ and moves to the target position during t_d. The base cart is decelerated after $t = 3(L - 0{\cdot}5)T_1 + t_d$ by the second pulse sequence during $3(L - 0{\cdot}5)T_2$ and stops at the target position. In this experiment T_1 for $h_1 = 0{\cdot}6$ m is 0·753 s, T_2 for $h_2 = 0{\cdot}4$ m is 0·474 s, t_d for the movement of the moving mass is 2 s, $\lambda = 1$, and $L = 1$. Thus, the total time taken for the task is $3T_1/2 + t_d + 3T_2/2 = 3{\cdot}84$ s. In this experiment, the high-frequency strain signal from $t = 3(L - 0{\cdot}5)T_1$ to $3(L - 0{\cdot}5)T_1 + t_d$ originates from the vertical movement of the moving mass.

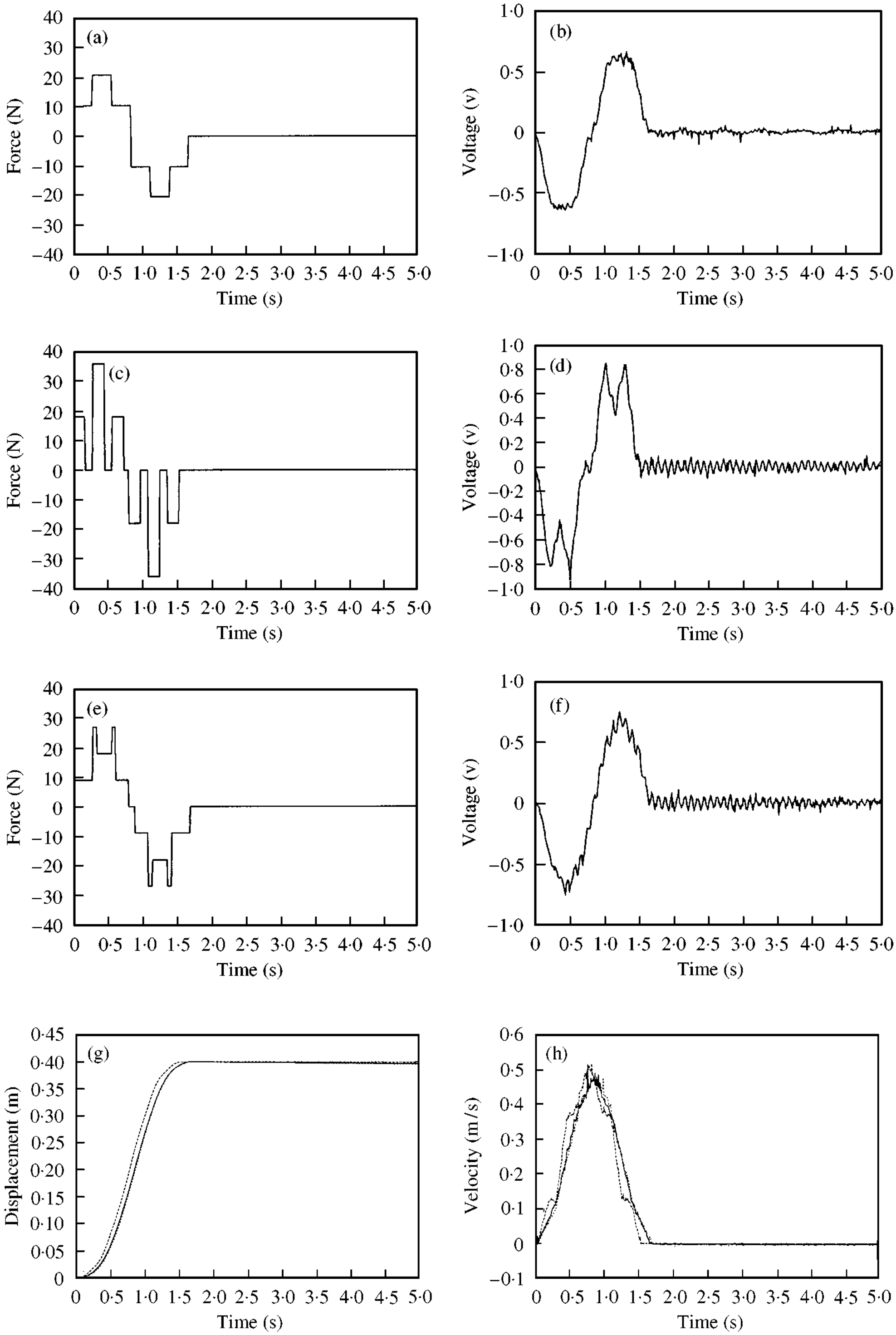

Figure 14. Experimental comparison of vibration suppression when $m = 5$ kg, $h = 0{\cdot}5$ m, and $x_f = 0{\cdot}4$ m: (a) $f(t)$ by proposed method, (b) strain signal by proposed method, (c) $f(t)$ by Teo's method, (d) strain signal by Teo's method, (e) $f(t)$ by Singer's method, (f) strain signal by Singer's method, (g) cart position, (h) cart velocity: ——, by proposed method; - - -, by Teo's ,method; ······, by Singer's method.

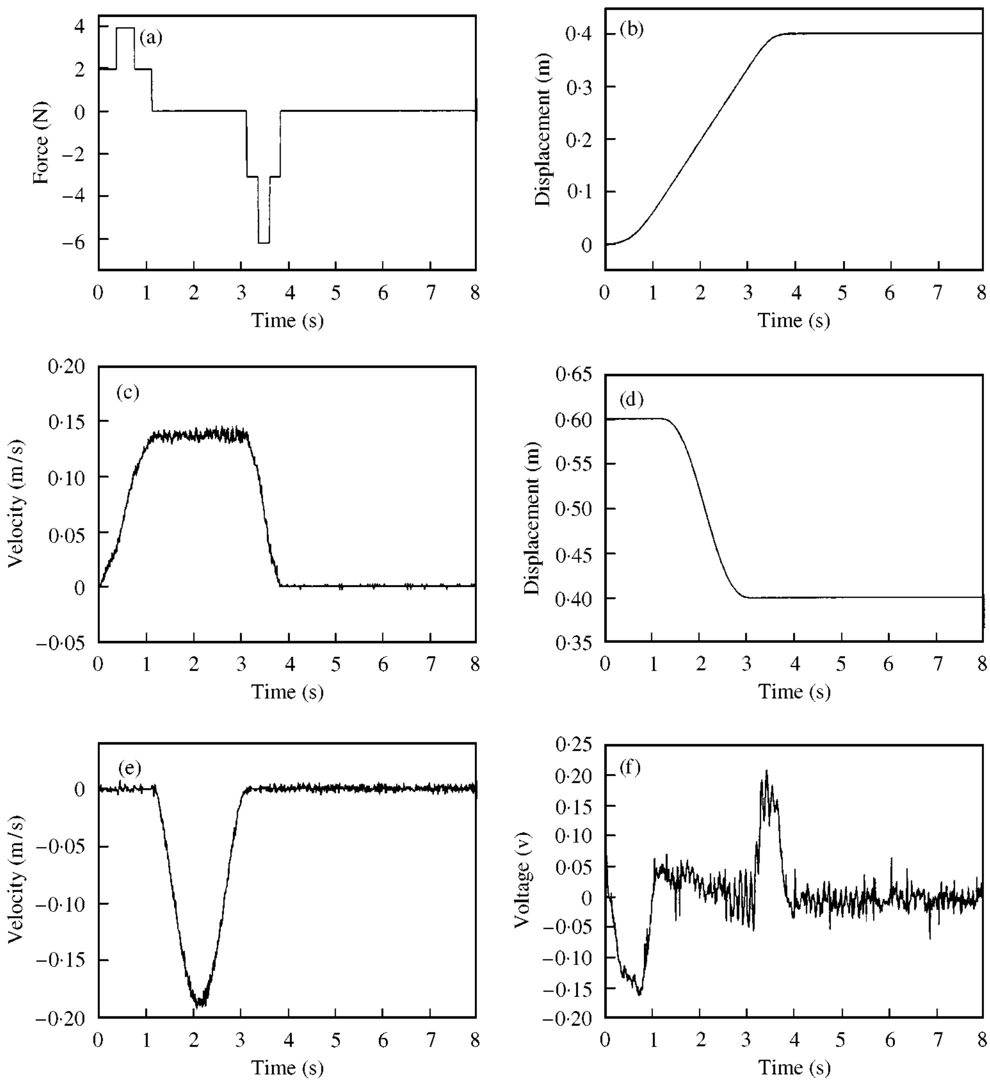

Figure 15. Experimental results of the PTP positioning of the moving mass from $(X, Y) = (0, 0{\cdot}6)$m to $(0{\cdot}4, 0{\cdot}4)$m: (a) shaped force, (b) cart position, (c) cart velocity, (d) moving mass position, (e) moving mass velocity, (f) strain signal.

5.5. INITIAL VIBRATION SUPPRESSION

All the input preshaping methods considered in this study cannot suppress the residual vibration of the beam when the beam has initial vibration. Initial vibration of the beam–mass–cart system with a concentrated mass can be suppressed by the proposed input preshaping. This can be done by applying an impulse which makes the inverse vibration as shown in Figure 16 [11, 12]. However, this method is not robust with respect to the change of the system parameters. This problem can be resolved by modifying the proposed input preshaping method.

In initial vibration suppression problem, it is important to know the natural frequency of the system and the amplitude of the force applied to the base cart. If the beam–mass system is excited by unknown force, the beam–mass system oscillates with a certain frequency.

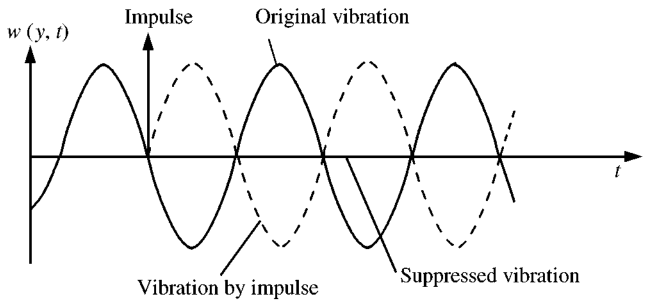

Figure 16. Initial vibration suppression without robustness.

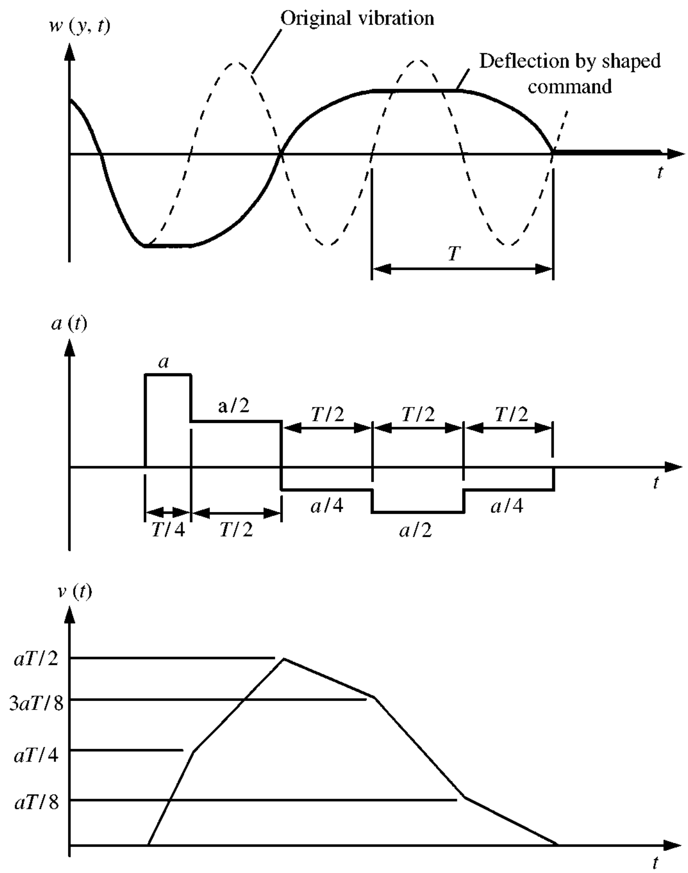

Figure 17. Initial vibration suppression with robustness using the proposed input preshaping method.

Therefore, if the vibration signal is measured by strain gauges, it is easy to know the frequency of the system using fast Fourier transformation (FFT). However, it is not very simple to determine the amplitude of the force applied to the base cart. It requires the static deflection model of the beam and some analytic results by modal analysis [20].

The deflection $w(y, t)$ can be obtained by the strain signal using a static deflection model. Using the obtained frequency of the system, it is simple to regenerate the vibration numerically and to match that with the actual one. Since the deflection $w(y, t)$ is expressed as

$$w(y, t) = \sum_{i=1}^{n} \phi_i(y) q_i(t), \tag{23}$$

if $w(y, t)$ is known, and if $\phi_i(y)$ is calculated using the model introduced in reference [20], then $q_i(t)$ can be obtained from equation (23). Further, if $q_i(t)$ can be known, the magnitude of force applied to the base cart can be obtained from

$$\ddot{q}_i(t) + \omega_i^2 q_i(t) = \beta_i f(t), \tag{24}$$

where ω_i is the damped natural frequency obtained from FFT, and β_i is the calculated value by the model introduced in reference [20]. For single-mode problem, $i = 1$ in the equation.

Figure 17 shows the concept of the initial vibration suppression using input preshaping. The obtained force $f(t)$ is applied to the system as shown in Figure 17. In Figure 17, the acceleration a is obtained from

$$a = \frac{f(t)}{M_t}, \tag{25}$$

where M_t is the total mass of the beam–mass–cart system. Since the deflection of the system is already estimated, it is easy to decide the time instant when the force should be applied.

In Figure 17, the first pulse with the magnitude of the acceleration a and period $T/4$ holds the deflection during $T/4$. The next pulse with the magnitude of the acceleration $a/2$ and period $T/2$ makes the deflection to disappear. The next pulse sequence with negative sign with respect to the former pulse sequence stops the base cart without residual vibration. The total distance of the base cart during this pulse sequences is

$$x_f = \frac{19}{32} a T^2. \tag{26}$$

Figure 18 shows the experimental results of initial vibration suppression when the concentrated mass $m = 5$ kg is located at $h = 0{\cdot}5$ m. The figure shows the drastic suppression of initial vibration by the shaped force.

5.6. SQUARE TRAJECTORY FOLLOWING A MOVING MASS

Using the concept proposed in the previous sections, the force profiles for the vibration suppression in following a square trajectory can be obtained. For example, if the task is following a square trajectory shown in Figure 19(a), the proposed pulse sequence method can be modified as seen in Figure 19(b). In Figure 19(b), T_1 is the period compatible to the height of the moving mass h_1, and T_2 is for h_2.

Experiments to follow square trajectories are performed using the proposed method. To certify the performance of the proposed input preshaping, the square trajectories of the moving mass with preshaping are compared with those without preshaping. The trajectories were obtained by taking pictures of the trajectories of the LED attached to the moving mass.

Figure 20 shows the trajectories of the moving mass when it moves along square trajectories without input preshaping. The moving mass moves from the origin

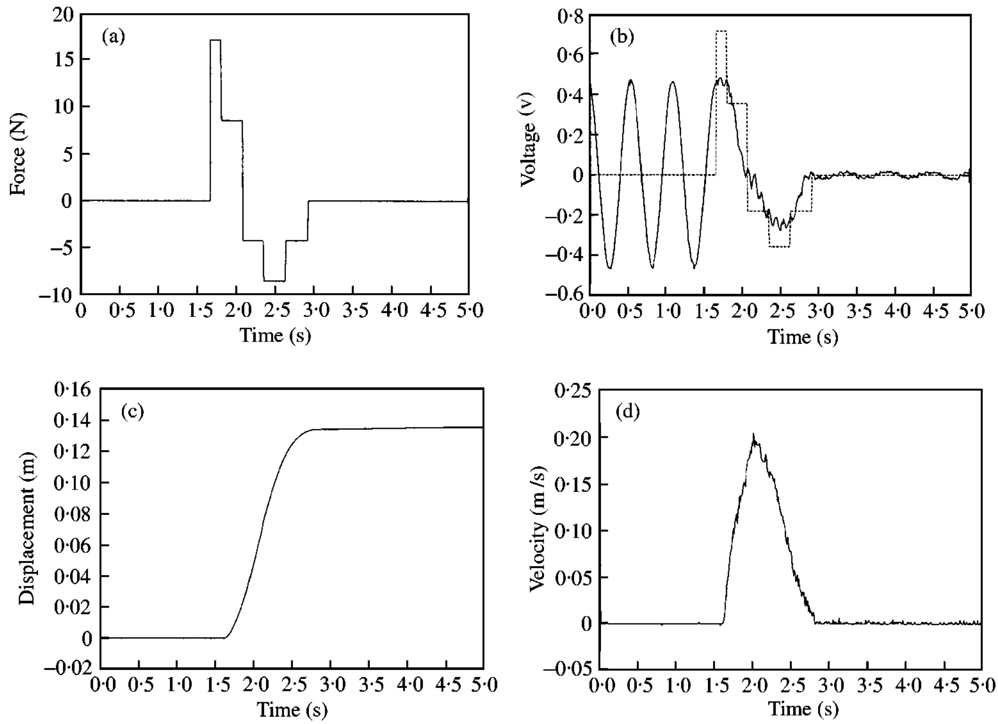

Figure 18. Experimental results for initial vibration suppression when $m = 5$ kg and $h = 0{\cdot}5$ m: (a) shaped command, (b) strain signal, (c) position of the base cart, (d) velocity of the base cart.

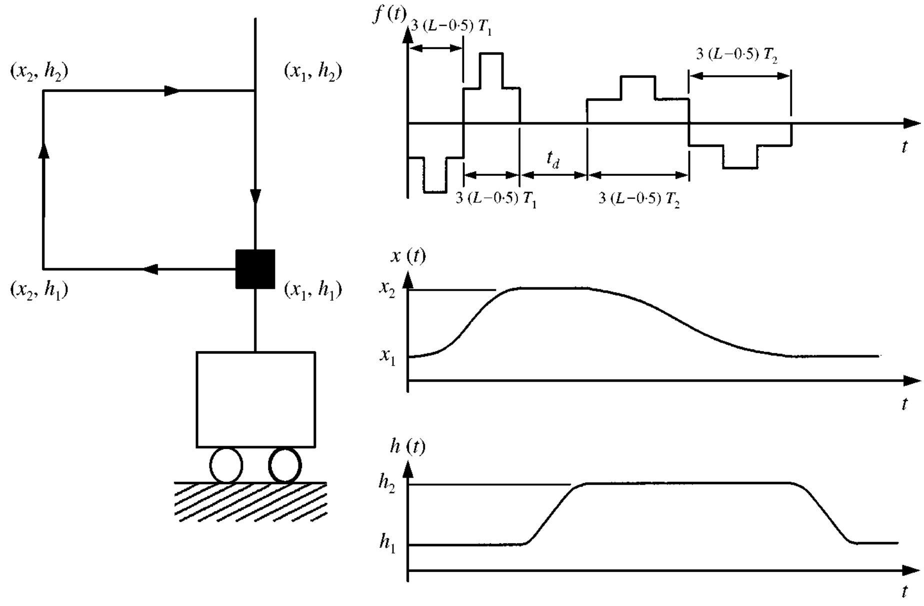

Figure 19. Input preshaping for square trajectory following: (a) task trajectory, (b) acceleration, cart position and moving mass position.

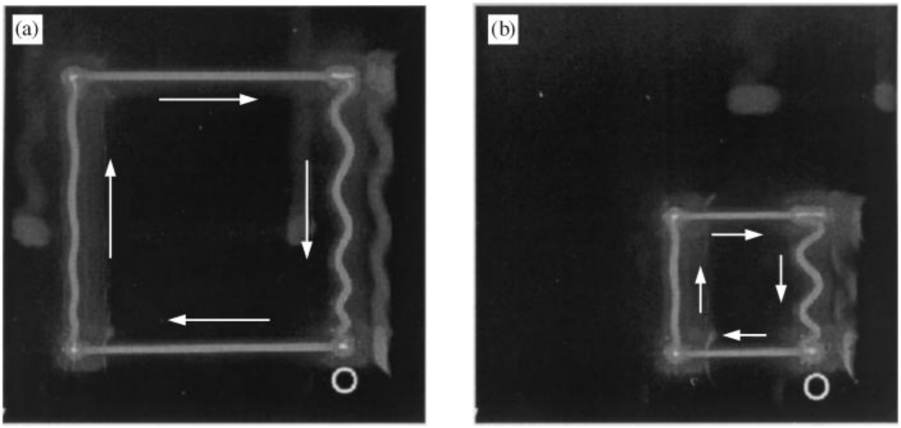

Figure 20. Trajectories of the moving mass without input preshaping: (a) square path (40 cm × 40 cm), (b) square path (20 cm × 20 cm).

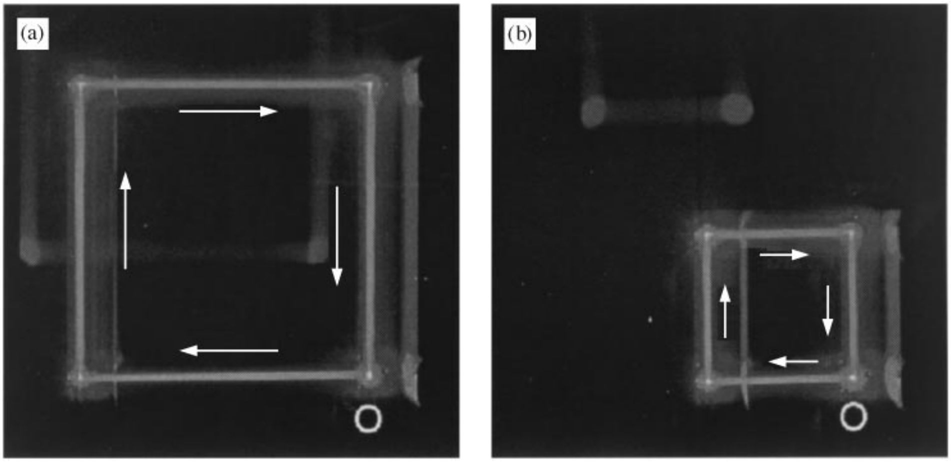

Figure 21. Trajectories of the moving mass with input preshaping: (a) square path (40 cm × 40 cm), (b) square path (20 cm × 20 cm).

$(X, Y) = (0, 0{\cdot}3)$ to the origin along 40 cm × 40 cm and 20 cm × 20 cm square trajectories in clockwise direction. As seen in Figure 20, the trajectories without input preshaping deviate from the given trajectories due to the vibration of the beam.

Figure 21 shows the trajectories of the moving mass when it follows the same trajectories in the previous experiments with the proposed input preshaping. As seen in Figure 21, the square trajectories obtained from the experiments show no vibration during their motion. The total time taken to follow the given square trajectories is $3T_1 + 3T_2 + 2t_d$. Therefore, it took $3 \times 0{\cdot}388$ s $+ 3 \times 0{\cdot}941$ s $+ 2 \times 4$ s $= 11{\cdot}906$ s, and $3 \times 0{\cdot}388$ s $+ 3 \times 0{\cdot}582$ s $+ 2 \times 2$ s $=$ $6{\cdot}91$ s for 40 cm × 40 cm and 20 cm × 20 cm trajectories respectively.

6. CONCLUDING REMARKS

In this study, a modified pulse sequence method with RIC was proposed to reduce single-mode residual vibration of a flexible beam fixed on a moving cart and carrying a concentrated or a moving mass. The performance of the proposed input preshaping methods was compared with the previous methods both by numerical simulations and experiments. All the methods considered in this study show satisfactory vibration reduction in short time. The proposed method, especially, requires less driving force and generates less deflection than by the other method though it shows longer settling time in some cases.

Using the proposed method, it was possible to suppress initial vibration of the beam–mass–cart system carrying a concentrated mass. Accurate PTP positioning of the moving mass without residual vibration is also carried out experimentally by modifying the proposed input preshaping method. Finally, the proposed input preshaping method was successfully applied to the system to follow square trajectories of the moving mass without residual vibration.

REFERENCES

1. R. H. Cannon Jr and E. Schmitz 1984 *The International Journal of Robotics Research* **3**, 325–338. Initial experiments on the end-point control of a flexible one-link manipulator.
2. P. T. Kotnik, S. Yurkovich and Ü. Özgüner 1988 *Journal of Robotic System* **5**, 181–196. Acceleration feedback for control of a flexible manipulator arm.
3. O. J. M. Smith 1958 *Feedback Control System*. New York: McGraw-Hill.
4. D. M. Aspinwall 1980 *ASME Journal of Dynamic Systems, Measurements, and Control* **102**, 3–6. Acceleration profiles for minimizing residual response.
5. C. J. Swigert 1980 *Journal of Guidance and Control* **3**, 460–467. Shaped torque techniques.
6. P. H. Meckl and W. P. Seering 1985 *ASME Journal of Vibration, Acoustics, Stress, and Reliability in Design* **107**, 38–46. Active damping in a three-axis robotic manipulator.
7. P. H. Meckl and W. P. Seering 1985 *ASME Journal of Vibration, Acoustics, Stress, and Reliability in Design* **107**, 378–382. Minimizing residual vibration for point-to-point motion.
8. P. H. Meckl and W. P. Seering 1986 *Proceedings of the American Control Conference, Seattle, WA*, 1913–1918. Feedforward control techniques to achieve fast settling time in robots.
9. P. H. Meckl and W. P. Seering 1988 *Proceedings of the IEEE International Conference on Robotics and Automation, Philadelphia, PA,* 1428–1433. Controlling velocity-limited systems to reduce residual vibration.
10. N. C. Singer and W. P. Seering 1988 *Proceedings of the IEEE International Conference on Robotics and Automation, Philadelphia, PA*, 1434–1439. Using acausal shaping techniques to reduce robot vibration.
11. N. C. Singer and W. P. Seering 1990 *ASME Journal of Dynamic Systems, Measurements, and Control* **112**, 76–82. Preshaping command inputs to reduce system vibration.
12. N. C. Singer and W. P. Seering 1989 *Proceedings of the NASA Space Telerobotics Conference, Pasadena, CA*, 53–62. Preshaping command inputs to reduce telerobotic system oscillations.
13. N. C. Singer and W. P. Seering 1990 *Proceedings of the American Control Conference, Vol.* **2**, 1738–1744. Experimental verification of command shaping methods for controlling residual vibration in flexible robots.
14. J. M. Hyde and W. P. Seering 1991 *Proceedings of the IEEE International Conference on Robotics and Automation, Sacramento, CA*, 2604–2608. Using input command pre-shaping to suppress multiple mode vibration.
15. S. P. Bhat and D. K. Miu 1991 *ASME Journal of Dynamic Systems, Measurement, and Control* **113**, 425–431. Solutions to point-to-point control problems using Laplace transform technique.
16. T. D. Tuttle and W. P. Seering 1994 *Proceedings of the American Control Conference, Baltimore, MA*, 2533–2537. A zero-placement technique for designing shaped inputs to suppress multiple-mode vibration.
17. T. Singh, M. F. Golnaraghi and R. H. Dubey 1994 *Journal of Sound and Vibration* **171**, 185–200. Sliding-mode/shaped-input control of flexible/rigid link robots.
18. C. L. Teo, C. J. Ong and M. Xu 1998 *Journal of Sound and Vibration* **211**, 157–177. Pulse input sequences for residual vibration reduction.
19. S. Park and Y. Youm 2000 *Journal of Sound and Vibration*. Vibrational motion of a moving elastic beam carrying a moving mass-analysis and experimental verification (in press).

20. S. PARK, W. K. CHUNG, Y. YOUM and J. W. LEE 2000 *Journal of Sound and Vibration* **230**, 591–615. Natural frequencies and open-loop responses of an elastic beam fixed on a moving cart and carrying an intermediate lumped mass.
21. B. K. KIM, H. T. CHOI, W. K. CHUNG and Y. H. CHANG 1999 *Proceedings of the IEEE International Symposium on Industrial Electronics,* 1045–1050. Robust optimal internal loop compensator design for motion control of precision linear motor.

APPENDIX A: NOMENCLATURE

a, a_1, a_2, a^*	acceleration of the base cart, m/s^2
a_{max}	maximum acceleration of the base cart, m/s^2
E	Young's modulus of the elastic beam, N/m^2
$f(t), f_1(t)$	force applied to the base cart, N
F_{max}	maximum force can be applied to the base cart, N
h, h_1, h_2	vertical position of the concentrated or moving mass, m
I	area moment of inertia of elastic beam, m^4
k_i	eigenfrequencies of the beam–mass–cart system
L	integer
m	mass of the concentrated or the moving mass, kg
m_b	mass of elastic beam, kg
M	mass of the base cart, kg
t_d	duration time between the first and second pulse trains, s
t_f	total time taken to reach the target position, s
t_w	time taken from 0 to the second pulse train, s
T, T'	period of the first mode vibration, s
T_1, T_2	period of the first mode vibration at $y = h_1$ and h_2, respectively, s
V_{max}	maximum velocity of the base cart, m/s
V_p	peak velocity of the base cart, m/s
$w(y, t)$	deflection of elastic beam at y, m
$w_h(t)$	deflection of elastic beam at $y = h$, m
$w_T(t)$	tip deflection of elastic beam, m
x_f	desired position of the base cart, m
Δt	duration time of pulse, s
ΔT	period of each impulse by Singer's method, s
ρ_0	mass per unit length of elastic beam, kg/m
ω_1	fundamental natural frequency of the beam–mass–cart system, rad/s, Hz
ζ	damping ratio of elastic beam.